Article

Effect of Ammonium Halide Additives on the Performance of Methyl Amine Based Perovskite Solar Cells

Do Yeon Heo [1], Zhengtang Luo [2,*] and Soo Young Kim [1,*]

[1] School of Chemical Engineering and Materials Science, Chung-Ang University, 84 Heukseok-ro, Dongjak-gu, Seoul 06974, Korea; doyoun0312@naver.com

[2] Department of Chemical and Biomolecular Engineering, the University of Hong Kong Science and Technology, Clear Water Bay, Kowloon, Hong Kong

[*] Correspondence: keztluo@ust.hk (Z.L.); sooyoungkim@cau.ac.kr (S.Y.K.)

Abstract: $CH_3NH_3PbI_{3-x}Cl_x$ species were fabricated as light-absorbing layers for perovskite solar cells (PSCs), by employing NH_4I, NH_4Br, and NH_4Cl as additives via annealing at 100 °C for different times. Solutions containing CH_3NH_3I, PbI_2, and $PbCl_2$ (4:1:1 molar ratio) in *N,N*-dimethylformamide were used to prepare perovskites with NH_4I, NH_4Br, and NH_4Cl as additives, at concentrations of 0.1 M and 0.3 M. The additives helped increase the grain size and reduce pinholes in the perovskite films, as confirmed by field-emission scanning electron microscopy. The X-ray diffraction profiles of $CH_3NH_3PbI_{3-x}Cl_x$ clearly showed peaks at 14° and 28° for the samples with additives, indicative of crystallinity. The best PSC performance with a power conversion efficiency of 9.13%, was achieved using 0.1 M NH_4I by annealing for 5 min, whereas the power conversion efficiency of the perovskite solar cells without additives was 5.40%.

Keywords: perovskite structure; perovskite solar cells; additive; ammonium halide

1. Introduction

In 2009, perovskite was first used as a sensitizer for light absorption in dye-sensitized solar cells (DSSCs), which gave a power conversion efficiency (PCE) of 3.8% [1]. Perovskite has an ABX_3 structure, where A, B, and X represent an organic cation, metal cation, and halide ion, respectively. Given perovskites have high absorption coefficients in the visible region, perovskite nanocrystals, especially $CH_3NH_3PbX_3$ (X = Br, I, Cl), are used as light absorbers. Park et al. achieved an improved PCE of 6.54% by using $CH_3NH_3PbI_3$ in DSSCs, in 2011 [2]. In 2012, $CH_3NH_3PbI_3$ and $CH_3NH_3PbI_2Cl$ were used as absorbers in solid-state hybrid solar cells to obtain PCEs of 9.7% and 10.9%, respectively [3,4], and research to increase the PCE of perovskite solar cells (PSCs) is ongoing [5–27]. In 2017, Seok and coworkers achieved a PCE of PSCs, as high as 22.1% [28].

The quality of the perovskite layer is important for increasing the PCE of PSCs [28–32]. Research to improve the quality of perovskite films by using additives is currently being pursued. For example, the addition of CH_3NH_3Cl [33], $CaCl_2$ [34], $InCl_3$ [35], NH_4Cl [36,37] etc., has been found to improve the morphology of perovskite films, thereby improving the performance of PSCs. PSCs with Cl-containing additives, showed high electrical conductivity and a long carrier diffusion length. Additives including, I^- also affect the performance of PSCs. When NaI [38], CuI [38], HI [39], and NH_4I [40] were used as additives, the PCEs of the resulting PSCs were 15.14%, 15.25%, 17.60%, and 18.31% respectively, which were higher compared to that of the PSCs without additives. Previous studies have shown that additives improve the morphology of perovskite films and increase the PCE of PSCs.

In this study, NH_4I, NH_4Br, and NH_4Cl were used as additives in the perovskite solution for film formation via spin-coating. The $CH_3NH_3PbI_{3-x}Cl_x$ perovskite solution for spin-coating was prepared in dimethylformamide (DMF). The concentration of the additives was varied, between 0.1 M and 0.3 M. After spin-coating, the perovskite films were annealed at 100 °C for 1, 5, 10, and 30 min. PSCs with an indium tin oxide (ITO)/poly(3,4-ethylenedioxythiophene):polystyrene sulfonate (PEDOT:PSS)/$CH_3NH_3PbI_{3-x}Cl_x$ perovskite/[6,6]-phenyl-C_{60} butyric acid methyl ester (PCBM)/bathocuproine (BCP)/LiF/Al device structure were fabricated. This study mainly shows device optimization through the change of various additives (NH_4I, NH_4Br, NH_4Cl), amounts of additives (0.1 M and 0.3 M), and annealing time (1, 5, 10, and 30 min), respectively. The characteristics of the $CH_3NH_3PbI_{3-x}Cl_x$ PSCs, were evaluated by controlling the annealing time and the concentration of additives, demonstrating that the PCE of the PSCs was improved by the additives. The details of the characteristics of the PSCs and the effects of the additives are discussed herein.

2. Experimental Details

2.1. Fabrication of $CH_3NH_3PbI_{3-x}Cl_x$ PSCs

ITO-coated glass (Woo Yang GMS, 15 Ω sq^{-1}) was used as the substrate. The glass was cleaned by successive ultrasonication in acetone, isopropyl alcohol, and deionized water for 15 min each. The substrate was then treated with UV-ozone for 15 min. A hole transport layer of PEDOT:PSS (Clevious) was spin-coated onto the glass substrate at 4000 rpm for 30 s, followed by heating at 150 °C for 15 min in air. The substrates were loaded into a N_2-filled glove box. As for synthesis of the $CH_3NH_3PbI_{3-x}Cl_x$ precursor, CH_3NH_3I, lead(II) iodide (PbI_2), and lead(II) chloride ($PbCl_2$) in a 4:1:1 molar ratio, were dissolved in an anhydrous DMF. Thereafter, 0.1 M or 0.3 M NH_4I, NH_4Br, and NH_4Cl were added to the solution. The precursor solution was then spin-coated onto the PEDOT:PSS layer at 4000 rpm for 30 s. The substrates were subsequently annealed at 100 °C for 1, 5, 10, and 30 min. A PCBM (Nanoholdings) solution (40 mg mL^{-1}) in chlorobenzene was then spin-coated on top of the perovskite film at 750 rpm for 15 s and the substrate was heated at 60 °C for 5 min. Subsequently, films of BCP (3 nm, Taewon Scientific CO, Seoul, Korea), LiF (1 nm, Taewon Scientific CO, Seoul, Korea), and Al (100 nm) were deposited on top of the electron transport layer (PCBM layer) under vacuum (<10^{-6} Torr) using a thermal evaporator, as shown in Figure 1. BCP and LiF, were used as hole blocking layers and Al was used as an electrode.
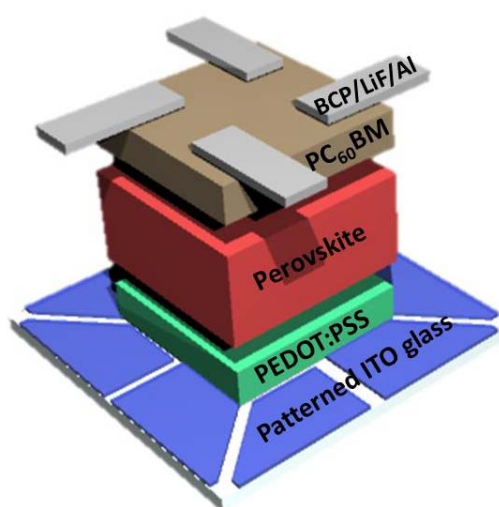

Figure 1. Schematic of inverted planar perovskite solar cells (PSC) device. The PSC is composed of ITO/PEDOT:PSS/$CH_3NH_3PbI_{3-x}Cl_x$/$PC_{60}BM$/BCP/LiF/Al. The single ITO substrate comprised four pixels and the illuminated areas of each pixel were 0.04 cm^2.

2.2. Characterizations

The X-ray diffraction (XRD, D8-Advance/Bruker-AXS (Billerica, MA, USA)) patterns were measured in an angle range of $2\theta = 10°$ to $50°$. The morphology of the films was shown through field emission scanning electron microscope (FE-SEM, Carl Zeiss, SIGMA (Kawasaki-shi, Japan)) images. The current-voltage (*J-V*) characteristics of PSCs were measured with a Keithley 2400 semiconductor parameter analyzer. The measurements were conducted under AM 1.5 G 100 mW/cm^2 illumination using an Oriel 150 W solar simulator. All devices were measured by masking the active area with a thin mask (0.04 cm^2). The *J-V* characteristics for all devices were measured at a voltage scan rate of 0.1 V s^{-1}.

3. Results and Discussion

We investigated the effect of the additives on crystallization of the $CH_3NH_3PbI_{3-x}Cl_x$ film through XRD, as shown in Figure 2. The perovskite films were prepared on PEDOT:PSS-coated ITO glass. The samples with and without additives were annealed at 100 °C for various times. NH_4I, NH_4Br, and NH_4Cl were used as additives. The XRD peaks of the $CH_3NH_3PbI_{3-x}Cl_x$ film are known to occur at 14° and 28° [36], as confirmed in Figure 2a. The XRD profiles of $CH_3NH_3PbI_{3-x}Cl_x$ without additives annealed for 1 min and 30 min, showed peaks at 13.8° and 28.0°. The samples annealed for 5 min and 10 min, showed peaks at 14.0° and 28.3°, and 14.1° and 28.4°, respectively. The sample annealed for 5 min exhibited the most intense peaks, indicating that the annealing time affected crystallization of the perovskite. The sample prepared with 0.1 M NH_4I and annealed for 5 min, also showed strong peaks at 14° and 28° (Figure 2b). Figure 2c shows the XRD peaks of the perovskite film prepared using 0.3 M NH_4I. Weak peaks were observed with annealing for 5 min and 30 min, but strong peaks were observed for the sample annealed at 10 min. However, the XRD peak of PbI_2 was observed at 12° [41] for the samples annealed for 1 min and 10 min. The peak of PbI_2 treated with 0.1 M NH_4Br and 0.3 M NH_4Br, is also shown in Figure 2d,e. The layers treated with NH_4Cl also showed XRD peaks at 14° and 28° (Figure 2f,g). The sample treated with 0.1 M NH_4Cl and annealed for 30 min exhibited a strong peak, whereas the samples annealed for 5 and 10 min exhibited a weak peak at 14°. All samples showed strong or weak peaks at 14° and 28°. Compared to, without additive, the XRD peaks of layers with additive showed strong peaks in all the layers, except for using 0.3 M NH_4I and 0.3 M NH_4Cl when annealed for 30 min. The layers using 0.1 M NH_4I, 0.3 M NH_4I, and 0.3 M NH_4Cl showed a stronger peak than the layer without additive, whilst the layers using 0.1 M NH_4Br, 0.3 M NH_4Br, and 0.1 M NH_4Cl showed weak peaks. All layers except 0.1 M NH_4I showed weaker peaks than the layer without additive, when annealed for 5 min. In the case of annealing for 1 min, all layers except 0.1 M and 0.3 M NH_4Cl showed a peak similar to the layer without additive. The samples treated with NH_4Cl showed a stronger peak than the sample without additive. Thus, it was found that the annealing time and the additives influenced crystallization of the $CH_3NH_3PbI_{3-x}Cl_x$ films.

Color changes in the perovskite layers were observed according to the annealing time and the additives. The $CH_3NH_3PbI_{3-x}Cl_x$ solution was combined with different concentrations of NH_4I, NH_4Br, or NH_4Cl as additives for spin coating. The samples were annealed at 100 °C for 1, 5, 10, or 30 min. Figure 3 shows optical images of the $CH_3NH_3PbI_{3-x}Cl_x$ layers, before and after annealing. Before annealing, the $CH_3NH_3PbI_{3-x}Cl_x$ films were brown, as shown in Figure 3a–c. There was only a slight difference depending on the additives. The color of the $CH_3NH_3PbI_{3-x}Cl_x$ films changed after annealing. As shown in Figure 3d, the samples prepared with 0.1 M NH_4I were nearly black regardless of the annealing time. However, those prepared with 0.3 M NH_4I were red and were similar to the layers prepared with 0.3 M NH_4Br (Figure 3e). After annealing the perovskite layer with 0.1 M NH_4Br for 1 min, the layer became green. However, the layer with 0.1 M NH_4Cl was a lighter green than that prepared with 0.1 M NH_4Br and annealed for 1 min. With the use of the 0.1 M additives, the color was similar to that of the reference cells after heat treatment. Therefore, it was confirmed that a small amount of additive had no significant effect on color. However, the effect of the annealing time in the crystallization of the perovskite could be confirmed through the different color of perovskite layers,

depending on the annealing time. The color of the perovskite layers treated with 0.3 M additives appeared to be affected by I$^-$, Br$^-$, and Cl$^-$, respectively. The use of 0.3 M NH$_4$Br and NH$_4$I with 1 min of annealing produced similar color changes, whereas NH$_4$Cl induced the formation of a greenish color. When the layers treated with 0.3 M additives were annealed for 5 min, those treated with NH$_4$I and NH$_4$Br were red, whereas the use of NH$_4$Cl produced a black phase, similar in color to the perovskite layer without additives. The use of 0.3 M additives and a longer annealing time gave rise to a black phase, similar to the CH$_3$NH$_3$PbI$_{3-x}$Cl$_x$ layer without additives.
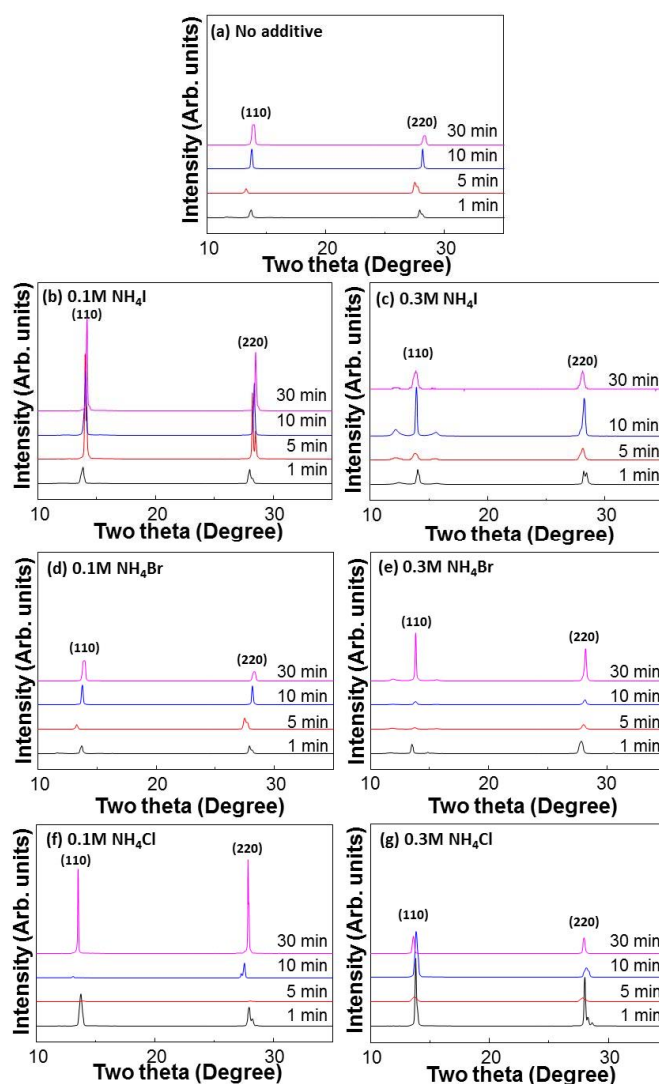

Figure 2. XRD spectra of CH$_3$NH$_3$PbI$_{3-x}$Cl$_x$ layers spin-coated on PEDOT:PSS layers. The CH$_3$NH$_3$PbI$_{3-x}$Cl$_x$ solutions used for spin-coating contained (**a**) no additive, (**b**) 0.1 M NH$_4$I, (**c**) 0.3 M NH$_4$I, (**d**) 0.1 M NH$_4$Br (**e**) 0.3 M NH$_4$Br (**f**) 0.1 M NH$_4$Cl, and (**g**) 0.3 M NH$_4$Cl respectively. The samples were annealed at 100 °C for different times (1, 5, 10, 30 min).

The color of the CH$_3$NH$_3$PbI$_{3-x}$Cl$_x$ layers, is illustrated in Figure 3. Notably, the surface quality and morphology have more influence on the performance of CH$_3$NH$_3$PbI$_{3-x}$Cl$_x$ PSCs, than the color of the perovskite layer [42]. The CH$_3$NH$_3$PbI$_{3-x}$Cl$_x$ films with additives were prepared on a PEDOT:PSS film. Figure 4 shows FE-SEM images of the perovskite layers annealed for different times, with different additives. When 0.1 M NH$_4$I was added to the CH$_3$NH$_3$PbI$_{3-x}$Cl$_x$ solution, the grain size increased and there were some pinholes compared to that of the sample annealed for 1 min (Figure 4a). Figure 4b shows that when 0.3 M NH$_4$I was added, the grain size increased as the annealing time increased,

and annealing for 30 min resulted in grains that were clustered with each other. As shown in Figure 4c,d, the FE-SEM images of the perovskite layer prepared with NH_4Br as the additive, showed an uneven surface. Particularly, the image of the sample prepared with 0.3 M NH_4Br showed a bright spot, which is estimated to be PbI_2, as confirmed by XRD. When NH_4Cl was used as the additive, there were many differences in the FE-SEM images depending on the concentration. Comparison of the samples prepared with 0.1 M NH_4Cl (Figure 4e) and 0.3 M NH_4Cl (Figure 4f), shows that there were large pinholes in the film prepared with 0.3 M NH_4Cl, which is expected to have a negative effect on the perovskite layer as the light absorbing layer in solar cells.

Figure 3. Optical images of $CH_3NH_3PbI_{3-x}Cl_x$ layers prepared with (**a**) NH_4I, (**b**) NH_4Br, and (**c**) NH_4Cl before annealing process and (**d**) NH_4I, (**e**) NH_4Br, (**f**) NH_4Cl after annealing process. The color change occurred after annealing.

Figure 5 shows the current density-voltage (*J-V*) curves of the $CH_3NH_3PbI_{3-x}Cl_x$ PSCs with NH_4I, NH_4Br, and NH_4Cl as additives. As a reference, a $CH_3NH_3PbI_{3-x}Cl_x$ PSC without any additive was also fabricated, as shown in Figure 5a. The open-circuit voltage (V_{OC}), short-circuit current (J_{SC}), fill factor (FF), and power conversion efficiency (PCE) of the PSCs employing the films with additives, are summarized in Table 1. The perovskite layers were annealed at 100 °C for different times. The annealing times were 1, 5, 10, and 30 min. For the reference $CH_3NH_3PbI_{3-x}Cl_x$ PSCs, the highest PCE of 5.40%, was achieved with the film annealed for 5 min. The corresponding J_{SC}, V_{OC}, and FF were 0.84, 9.45, and 0.68, respectively. The same PCE (4.64%) was achieved with annealing times of 10 min and 30 min. On the other hand, when the $CH_3NH_3PbI_{3-x}Cl_x$ layer was annealed for 1 min, the J_{SC}, V_{OC}, FF, and PCE values declined significantly to 1.64 mA cm^{-2}, 0.81 V, 0.15, and 0.20%, respectively. Thus, it could be deduced that the cubic perovskite was not formed when the perovskite layer was annealed for 1 min. However, the PCE of the $CH_3NH_3PbI_{3-x}Cl_x$ PSCs employing the films with additives was higher than that of the PSCs employing the films without additives annealed for 1 min. The V_{OC}, J_{SC}, FF, and PCE of 0.86 V, 12.2 mA cm^{-2}, 0.67, and 7.31%, respectively achieved using 0.1 M NH_4I were significantly higher values. When 0.1 M NH_4I was used as the additive and the perovskite layer was annealed for 5 min, the highest efficiency was obtained. The corresponding V_{OC}, J_{SC}, FF, and PCE values were 0.78 V, 16.3 mA cm^{-2}, 0.72, and 9.13%, respectively. The PCE was 69% higher than that of the PSCs employing the perovskites without additives, under the same conditions. It was confirmed that the PCE decreased with longer heat treatment. When the concentration of NH_4I was increased to 0.3 M, the PSC performance declined. Unlike the case with 0.1 M NH_4I, where the highest PCE was achieved with the film annealed for 5 min, the highest PCE attained with 0.3 M NH_4I was achieved with annealing for 10 min. The corresponding V_{OC}, J_{SC}, FF, and PCE were 0.79 V, 10.8 mA cm^{-2}, 6.70, and 6.06%, respectively. Thus, it was confirmed that the higher the concentration

of NH_4I as the additive, the longer the required annealing time. The $CH_3NH_3PbI_{3-x}Cl_x$ PSCs with the NH_4Br-treated film showed remarkably low performance when 0.3 M NH_4Br was added, compared to 0.1 M NH_4Br. The V_{OC}, J_{SC}, FF, and PCE values of the PSCs employing the 0.1 M NH_4Br-treated film were 0.85 V, 11.7 mA cm^{-2}, 0.66, and 6.57%, respectively, whereas that of the PSCs with the 0.3 M NH_4Br-treated films were 0.87 V, 3.09 mA cm^{-2}, 0.23, and 0.61%, respectively, when annealing was performed for 5 min. When 0.1 M NH_4Br was used as the additive, the Br^- in NH_4Br did not affect the $CH_3NH_3PbI_{3-x}Cl_x$ structure significantly. However, when 0.3 M NH_4Br was added, it is considered that Br^- bonded with $CH_3NH_3PbI_{3-x}Cl_x$ and disrupted the cubic structure. On the other hand, the performance parameters of the PSCs were higher when NH_4I and NH_4Cl were used as additives. It is considered that I^- and Cl^- helped to maintain the cubic structure of the perovskite. The V_{OC}, J_{SC}, and FF were 0.80 V, 15.1 mA cm^{-2}, and 0.67, respectively, for the highest PCE of 8.13%, achieved with 0.1 M NH_4Cl. With the use of 0.3 M NH_4Cl, the V_{OC}, J_{SC}, FF, and PCE values were 0.67 V, 14.4 mA cm^{-2}, 0.63, and 6.13%, respectively. The performance of the $CH_3NH_3PbI_{3-x}Cl_x$ PSCs employing the films treated with NH_4I, NH_4Br, and NH_4Cl as additives was investigated. The additive is related to the grain size of perovskite. As a result, the diffusion length of the active layer became longer as the grain size increased, confirming that J_{SC} and PCE were increased. It can also be seen that a small amount of additive was more effective than a large amount. In addition, it was confirmed that the annealing time affected the characteristics of the perovskite solar cells due to the decrease in efficiency, as the annealing time became longer.
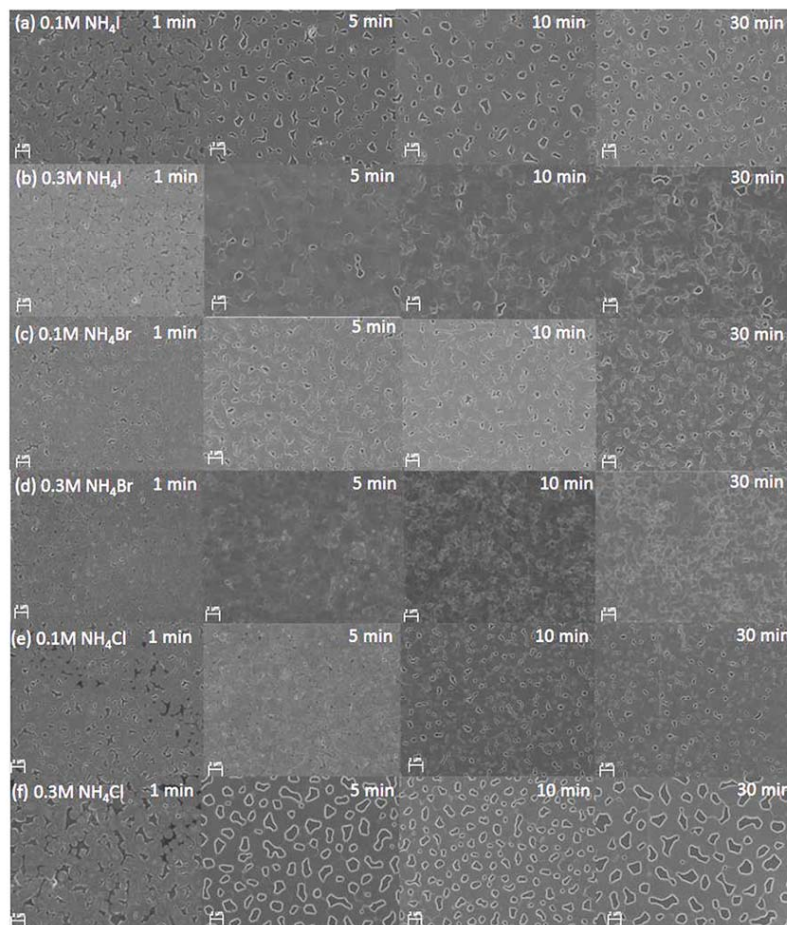

Figure 4. FE-SEM images of $CH_3NH_3PbI_{3-x}Cl_x$ layers coated on PEDOT:PSS layers. The $CH_3NH_3PbI_{3-x}Cl_x$ solutions used for spin-coating contained (**a**) 0.1 M NH_4I, (**b**) 0.3 M NH_4I, (**c**) 0.1 M NH_4Br, (**d**) 0.3 M NH_4Br, (**e**) 0.1 M NH_4Cl, and (**f**) 0.3 M NH_4Cl, respectively. The samples were annealed at 100 °C for different times (1, 5, 10, and 30 min). The scale bar is 2 μm.
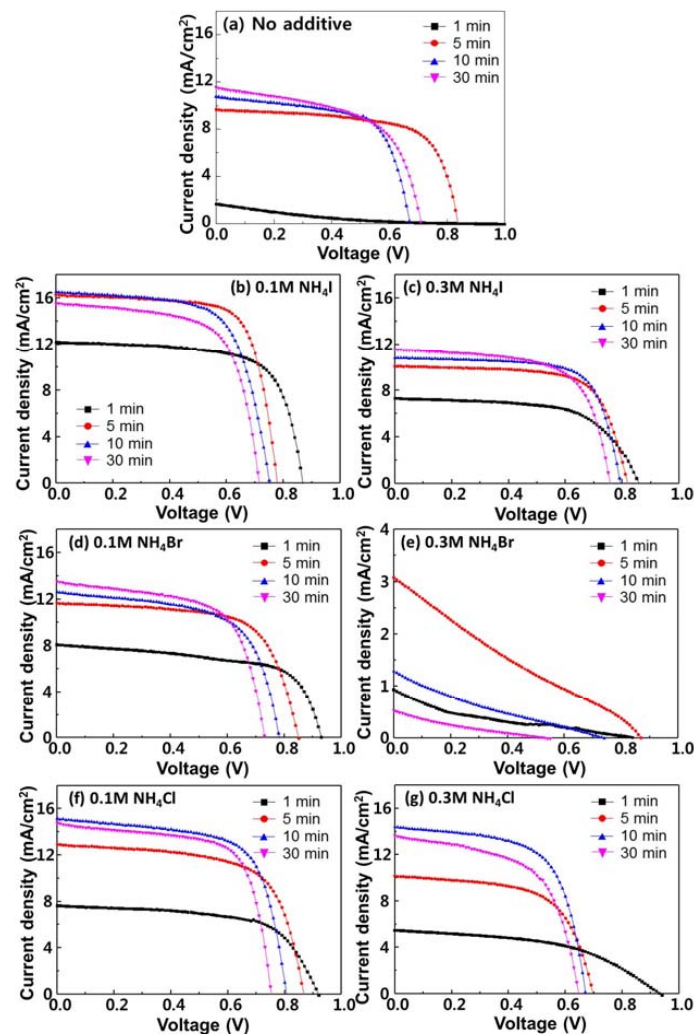
Figure 5. (**a**) Current density-voltage curves of $CH_3NH_3PbI_{3-x}Cl_x$ PSCs, without any additives. The samples were annealed at 100 °C for 1, 5, 10, and 30 min, respectively. The optimal annealing time was 10 min with PCE 5.40%. Current density-voltage curves of $CH_3NH_3PbI_{3-x}Cl_x$ PSCs with additives of (**b**) 0.1 M NH_4I, (**c**) 0.3 M NH_4I, (**d**) 0.1 M NH_4Br, (**e**) 0.3 M NH_4Br, (**f**) 0.1 M NH_4Cl, and (**g**) 0.3 M NH_4Cl, respectively. The maximum average PCE values of the $CH_3NH_3PbI_{3-x}Cl_x$ PSCs with NH_4I, NH_4Br, and NH_4Cl additives are 9.13, 6.57, and 8.13%, respectively.

Table 1. Photovoltaic performance of $CH_3NH_3PbI_{3-x}Cl_x$ PSCs with films treated with NH_4I, NH_4Br, and NH_4Cl additives. The average values are from 20 cells for each type of device, with AM 1.5 G solar irradiation.

Additives	Annealing Time (min)	V_{OC} (V)	J_{SC} (mA/cm^2)	FF	PCE (%)
NH_4I, 0.1 M	1	0.86	12.2	0.67	7.31
	5	0.78	16.3	0.72	9.13
	10	0.75	16.5	0.66	8.20
	30	0.71	15.6	0.66	7.31
NH_4I, 0.3 M	1	0.86	7.31	0.62	3.87
	5	0.82	10.1	0.69	5.72
	10	0.79	10.8	0.70	6.06
	30	0.76	11.6	0.65	5.67
NH_4Br, 0.1 M	1	0.93	8.08	0.62	4.69
	5	0.85	11.7	0.66	6.57
	10	0.78	12.6	0.62	4.69
	30	0.73	13.6	0.63	6.23

Table 1. *Cont.*

Additives	Annealing Time (min)	V_{OC} (V)	J_{SC} (mA/cm^2)	FF	PCE (%)
NH$_4$Br, 0.3 M	1	0.91	0.91	0.19	0.15
	5	0.87	3.09	0.23	0.61
	10	0.73	1.29	0.20	0.19
	30	0.53	0.53	0.18	0.051
NH$_4$Cl, 0.1 M	1	0.92	7.63	0.63	4.42
	5	0.87	12.9	0.65	7.30
	10	0.80	15.1	0.67	8.13
	30	0.75	14.8	0.68	7.56
NH$_4$Cl, 0.3 M	1	0.93	5.25	0.51	2.49
	5	0.70	10.2	0.61	4.36
	10	0.67	14.4	0.63	6.13
	30	0.64	13.1	0.60	5.11
No additive	1	0.81	1.64	0.15	0.20
	5	0.84	9.45	0.68	5.40
	10	0.67	10.8	0.64	4.64
	30	0.71	11.6	0.56	4.64

4. Conclusions

In summary, an innovative approach by adding the methylammonium halide to enhance the performance of CH$_3$NH$_3$PbI$_{3-x}$Cl$_x$ PSCs was developed. CH$_3$NH$_3$PbI$_{3-x}$Cl$_x$ films were fabricated for one-step coating with perovskite solution, using NH$_4$I, NH$_4$Br, and NH$_4$Cl as additives. The XRD patterns and FE-SEM images of the CH$_3$NH$_3$PbI$_{3-x}$Cl$_x$ films with additives generally, showed the presence of strong peaks at 14° and 28°, and an increase in the grain size of the perovskite with additives, but some pinholes were present. Investigation of the photovoltaic performance of the PSCs with additives, showed that the PCE of the CH$_3$NH$_3$PbI$_{3-x}$Cl$_x$ PSCs with the 0.3 M NH$_4$Br-treated films was lower than that of the PSCs employing films without additives. It is proposed that, Br$^-$ from NH$_4$Br substituted the I$^-$ of CH$_3$NH$_3$PbI$_{3-x}$Cl$_x$, thereby disrupting its structure, and I$^-$ reacted with Pb$^+$ to form PbI$_2$, leading to a decrease in the PCE. The highest PCE of the PSCs employing the films treated with 0.1 M NH$_4$I was 9.13%, which was 69% higher than that of the PSCs employing films without any additive. It was confirmed that small amounts of NH$_4$I, NH$_4$Br, and NH$_4$Cl maintain structure and improve the properties of CH$_3$NH$_3$PbI$_{3-x}$Cl$_x$ PSCs. These results indicated that the additives, especially 0.1 M NH$_4$I, were effective in improving the characteristics of CH$_3$NH$_3$PbI$_{3-x}$Cl$_x$ PSCs.

References

1. Kojima, A.; Teshima, K.; Shirai, K.; Miyasaka, T. Organometal Halide Perovskites as Visible-Light Sensitizers for Photovoltaic Cells. *J. Am. Chem. Soc.* **2009**, *131*, 6050–6051. [CrossRef] [PubMed]
2. Im, J.-H.; Lee, C.-R.; Lee, J.-W.; Park, S.-W.; Park, N.-G. 6.5% efficient perovskite quantum-dot-sensitized solar cell. *Nanoscale* **2011**, *3*, 4088–4093. [CrossRef] [PubMed]
3. Kim, H.-S.; Lee, C.-R.; Im, J.-H.; Lee, K.-B.; Moehl, T.; Marchioro, A.; Moon, S.-J.; Humphry-Baker, R.; Yum, J.-H.; Moser, J.E.; et al. Lead Iodide Perovskite Sensitized All-Solid-State Submicron Thin Film Mesoscopic Solar Cell with Efficiency Exceeding 9%. *Sci. Rep.* **2012**, *2*, 591. [CrossRef] [PubMed]

4. Lee, M.M.; Teuscher, J.; Miyasaka, T.; Murakami, T.N.; Snaith, H.J. Efficient Hybrid Solar Cells Based on Meso-Superstructured Organometal Halide Perovskites. *Science* **2012**, *338*, 643–647. [CrossRef] [PubMed]

5. Le, Q.V.; Nguyen, T.P.; Choi, K.S.; Cho, Y.-H.; Hong, Y.J.; Kim, S.Y. Dual use of tantalum disulfides as hole and electron extraction layers in organic photovoltaic cells. *Phys. Chem. Chem. Phys.* **2014**, *16*, 25468–25472. [CrossRef] [PubMed]

6. Lee, C.Y.; Le, Q.V.; Kim, C.; Kim, S.Y. Use of silane-functionalized graphene oxide on organic photovoltaic cells and organic light-emitting diodes. *Phys. Chem. Chem. Phys.* **2015**, *17*, 9369–9374. [CrossRef] [PubMed]

7. Le, Q.V.; Shin, J.W.; Jung, J.-H.; Park, J.; Ozturk, A.; Kim, S.Y. Control of the Crystal Growth Shape in $CH_3NH_3PbBr_3$ Perovskite Materials. *J. Nanosci. Nanotechnol.* **2017**, *17*, 8169–8174. [CrossRef]

8. Huang, J.; Wang, M.; Ding, L.; Yang, Z.; Zhang, K. Hydrobromic acid assisted crystallization of $MAPbI_{3-x}Cl_x$ for enhanced power conversion efficiency in perovskite solar cells. *RSC Adv.* **2016**, *6*, 55720–55725. [CrossRef]

9. Hasani, A.; Gavgani, J.N.; Pashaki, R.M.; Baseghi, S.; Salehi, A.; Heo, D.; Kim, S.Y.; Mahyari, M. Poly(3,4 ethylenedioxythiophene):Poly(Styrenesulfonate)Iron(III) Porphyrin Supported on S and N Co-Doped Graphene Quantum Dots as a Hole Transport Layer in Polymer Solar Cells. *Sci. Adv. Mater.* **2017**, *9*, 1616–1625. [CrossRef]

10. Le, Q.V.; Choi, J.-Y.; Kim, S.Y. Recent advances in the application of two-dimensional materials as charge transport layer in organic and perovskite solar cells. *FlatChem* **2017**, *2*, 54–66. [CrossRef]

11. Kim, Y.G.; Kwon, K.C.; Le, Q.V.; Hong, K.; Jang, H.W.; Kim, S.Y. Atomically thin two-dimensional materials as hole extraction layers in organolead halide perovskite photovoltaic cells. *J. Power Source* **2016**, *319*, 1–8. [CrossRef]

12. Kwon, K.C.; Hong, K.; Le, Q.V.; Lee, S.Y.; Choi, J.; Kim, K.-B.; Kim, S.Y.; Jang, H.W. Inhibition of Ion Migration for Reliable Operation of Organolead Halide Perovskite-Based Metal/Semiconductor/Metal Broadband Photodetectors. *Adv. Fun. Mater.* **2016**, *26*, 4213–4222. [CrossRef]

13. Kim, Y.G.; Kim, T.-Y.; Oh, J.H.; Choi, K.S.; Kim, Y.-J.; Kim, S.Y. Cesium lead iodide solar cells controlled by annealing temperature. *Phys. Chem. Chem. Phys.* **2017**, *19*, 6257–6263. [CrossRef] [PubMed]

14. Le, Q.V.; Nguyen, T.P.; Jang, H.W.; Kim, S.Y. The use of UV/ozone-treated MoS_2 nanosheets for extended air stability in organic photovoltaic cells. *Phys. Chem. Chem. Phys.* **2014**, *16*, 13123–13128. [CrossRef] [PubMed]

15. Wang, Z.X.; Zhan, X.Y.; Wang, Y.J.; Muhammad, S.; Huang, Y.; He, J. A flexible UV nanosensor based on reduced graphene oxide decorated ZnO nanostructures. *Nanoscale* **2012**, *4*, 2678–2684. [CrossRef] [PubMed]

16. Chen, Q.; Zhou, H.; Hong, Z.; Luo, S.; Duan, H.-S.; Wang, H.-H.; Liu, Y.; Li, G.; Yang, Y. Planar heterojunction perovskite solar cells via vapor-assisted solution process. *J. Am. Chem. Soc.* **2013**, *136*, 622–625. [CrossRef] [PubMed]

17. Xiao, M.; Huang, F.; Huang, W.; Dkhissi, Y.; Zhu, Y.; Etheridge, J.; Gray-Weale, A.; Bach, U.; Cheng, Y.-B.; Spiccia, L. A Fast Deposition-Crystallization Procedure for Highly Efficient Lead Iodide Perovskite Thin-Film Solar Cells. *Angew. Chem.* **2014**, *126*, 1–7. [CrossRef]

18. Li, G.; Shrotriya, V.; Huang, J.; Yao, Y.; Moriarty, T.; Emery, K.; Yang, Y. High-efficiency solution processable polymer photovoltaic cells by self-organization of polymer blends. *Nat. Mater.* **2005**, *4*, 864–868. [CrossRef]

19. Sista, S.; Park, M.-H.; Hong, Z.; Wu, Y.; Hou, J.; Kwan, W.L.; Li, G.; Yang, Y. Highly Efficient Tandem Polymer Photovoltaic Cells. *Adv. Mater.* **2010**, *22*, 380–383. [CrossRef] [PubMed]

20. Lee, Y.H.; Luo, J.; Son, M.-K.; Gao, P.; Cho, K.T.; Seo, J.; Zakeeruddin, S.M.; Grätzel, M.; Nazeeruddin, M.K. Enhanced Charge Collection with Passivation Layers in Perovskite Solar Cells. *Adv. Mater.* **2016**, *28*, 3966–3972. [CrossRef] [PubMed]

21. Liu, X.; Wang, H.; Yang, T.; Zhang, W.; Gong, X. Solution-Processed Ultrasensitive Polymer Photodetectors with High External Quantum Efficiency and Detectivity. *ACS Appl. Mater. Interfaces* **2012**, *4*, 3701–3705. [CrossRef] [PubMed]

22. Jeon, N.J.; Noh, J.H.; Kim, Y.C.; Yang, W.S.; Ryu, S.; Seok, S.I. Solvent engineering high-performance inorganic-organic hybrid perovskite solar cells. *Nat. Mater.* **2014**, *13*, 897–903. [CrossRef] [PubMed]

23. Fu, X.W.; Liao, Z.M.; Zhou, Y.B.; Wu, H.C.; Bie, Y.Q.; Xu, J.; Yu, D.-P. Graphene/ZnO nanowire/graphene vertical structure based fast-response ultraviolet photodetector. *Appl. Phys. Lett.* **2012**, *100*, 223114. [CrossRef]

24. Kim, A.; Won, Y.; Woo, K.; Kim, C.H.; Jooho, M. Highly Transparent Low Resistance ZnO/Ag Nanowire/ZnO Composite Electrode for Thin Film Solar Cells. *ACS Nano* **2013**, *7*, 1081–1091. [CrossRef] [PubMed]

25. Mutiso, R.M.; Sherrott, M.C.; Rathmell, A.R.; Wiley, B.J.; Winey, K.I. Integrating Simulations and Experiments to Predict Sheet Resistance and Optical Transmittance in Nanowire Films for Transparent Conductors. *ACS Nano* **2013**, *7*, 7654–7663. [CrossRef] [PubMed]

26. Dualeh, A.; Moehl, T.; Gao, P.; Nazeeruddin, M.K.; Grätzel, M. Effect of Annealing Temperature on Film Morphology of Organic-Inorganic Hybrid Perovskite Solid-State Solar Cells. *Funct. Mater.* **2014**, *24*, 3250–3258. [CrossRef]

27. Carnie, M.J.; Charbonneau, C.; Davies, M.L.; Troughton, J.; Watson, T.M.; Wojciechowski, K.; Snaith, H.; Worsley, D.A. A one-step low temperature processing route for organolead halide perovskite solar cells. *Chem. Commun.* **2013**, *49*, 7893–7895. [CrossRef] [PubMed]

28. Yang, W.S.; Park, B.-K.; Jung, E.H.; Jeon, N.J.; Kim, Y.C.; Lee, D.U.; Shin, S.S.; Seo, J.; Kim, E.K.; Noh, J.H.; et al. Iodide management in formamidinium-lead-halide–based perovskite layers for efficient solar cells. *Science* **2017**, *356*, 1376–1379. [CrossRef] [PubMed]

29. McMeekin, D.P.; Sadoughi, G.; Rehman, W.; Eperon, G.E.; Saliba, M.; HöNrantner, M.T.; Haghighirad, A.; Sakai, N.; Korte, L.; Rech, B.; et al. A mixed-cation lead mixed-halide perovskite absorber for tandem solar cells. *Science* **2016**, *351*, 151–155. [CrossRef] [PubMed]

30. Li, X.; Ibrahim Dar, M.; Yi, C.; Luo, J.; Tschumi, M.; Zakeeruddin, S.M.; Nazeeruddin, M.K.; Han, H.; Grätzel, M. Improved performance and stability of perovskite solar cells by crystal crosslinking with alkylphosphonic acid ω-ammonium chlorides. *Nat. Chem.* **2015**, *7*, 703–711. [CrossRef] [PubMed]

31. Heo, J.H.; Song, D.H.; Im, S.H. Planar $CH_3NH_3PbBr_3$ Hybrid Solar Cells with 10.4% Power Conversion Efficiency, Fabricated by Controlled Crystallization in the Spin-Coating Process. *Adv. Mater.* **2014**, *26*, 8179–8183. [CrossRef] [PubMed]

32. Zhao, Y.; Zhu, K. Three-step sequential solution deposition of PbI_2-free $CH_3NH_3PbI_3$ perovskite. *J. Mater. Chem. A* **2015**, *3*, 9086–9091. [CrossRef]

33. Docampo, P.; Hanusch, F.-C.; Stranks, S.-D.; Döblinger, M.; Feckl, J.-M.; Ehrensperger, M.; Minar, N.-K.; Johnston, M.-B.; Snaith, H.-J.; Bein, T. Solution Depositon-Conversion for Planar Heterojunction Mixed Halide Perovskite Solar Cell. *Adv. Energy Mater.* **2014**, *4*, 1400355. [CrossRef]

34. Chen, Y.; Zhao, Y.; Liang, Z. Nonvolatile chlorinated additives adversely influence $CH_3NH_3PbI_3$ based planar solar cells. *J. Mater. Chem. A* **2015**, *3*, 9137–9140. [CrossRef]

35. Wang, Z.-K.; Li, M.; Yang, Y.-G.; Hu, Y.; Ma, H.; Gao, X.-Y.; Liao, L.-S. High Efficiency Pb-In Binary Metal Perovskite Solar Cells. *Adv. Mater.* **2016**, *28*, 6695–6703. [CrossRef] [PubMed]

36. Zuo, C.; Ding, L. An 80.11% FF record achieved for perovskite solar cells by using the NH_4Cl additive. *Nanoscale* **2014**, *6*, 9935–9938. [CrossRef] [PubMed]

37. Oku, T.; Ohishi, Y.; Ueoka, N. Highly (100)-oriented $CH_3CH_3PbI_3(Cl)$ perovskite solar cells prepared with NH_4Cl using an air blow method. *RSC Adv.* **2018**, *8*, 10389–10395. [CrossRef]

38. Abdi-Jalebi, M.; Dar, M.-I.; Sadhanala, A.; Senanayak, S.-P.; Franckevičius, M.; Arora, N.; Hu, Y.; Nazeeruddin, M.-K.; Zakeeruddin, S.-M.; Grätzel, M.; Friend, R.-H. Impact of Monovalent Cation Halide Additives on the Structural and Optoelectronic Properties of $CH_3NH_3PbI_3$ perovskite. *Adv. Energy Mater.* **2016**, *6*, 1502472. [CrossRef]

39. Heo, J.-H.; Song, D.-H.; Han, H.-J.; Kim, S.-Y.; Kim, J.-H.; Kim, D.; Shin, H.-W.; Ahn, T.-K.; Wolf, C.; Lee, T.; et al. Planar $CH_3NH_3PbI_3$ Perovskite Solar Cells with Constant 17.2% Average Power Conversion Efficiency Irrespective of the Scan Rate. *Adv. Mater.* **2015**, *27*, 3424–3430. [CrossRef] [PubMed]

40. Zheng, H.; Liu, G.; Zhu, L.; Ye, J.; Zhang, X.; Alsaedi, A.; Hayat, T.; Pan, X.; Dai, S. Enhanced Performance and Stability of Perovskite Solar Cells Using NH_4I Interfacial Modifier. *ACS Appl. Mater. Interfaces* **2017**, *9*, 41006–41013. [CrossRef] [PubMed]

41. Zhou, H.; Chen, Q.; Li, G.; Luo, S.; Song, T.-B.; Duan, H.-S.; Hong, Z.; You, J.; Liu, Y.; Yang, Y. Interface engineering of highly efficient perovskite solar cells. *Science* **2014**, *345*, 542–546. [CrossRef] [PubMed]

42. Huang, J.; Wang, M.; Ding, L.; Igbari, F.; Yao, X. Efficiency enhancement of $MAPbI_xCl_{3-x}$ based perovskite solar cell by modifying the TiO_2 interface with Silver Nanowires. *Sol. Energy* **2016**, *130*, 273–280. [CrossRef]